Multiple Camera Human Detection and Tracking Inside a Robotic Cell

An Approach based on Image Warping, Computer Vision, K-d Trees and Particle Filtering

Matteo Ragaglia, Luca Bascetta and Paolo Rocco
Dipartimento di Elettronica, Informazione e Bioingegneria,
Politecnico di Milano, Piazza Leonardo da Vinci - 32, 20133, Milan, Italy

Keywords: Human Detection and Tracking, Robotic Cell Supervision, Computer Vision, Image Warping, Background/Foreground Segmentation, K-d Tree, Particle Filtering.

Abstract: In an industiral scenario the capability to detect and track human workers entering a robotic cell represents a fundamental requirement to enable safe and efficient human-robot cooperation. This paper proposes a new approach to the problem of Human Detection and Tracking based on low-cost commercial RGB surveillance cameras, image warping techniques, computer vision algorithms, efficient data structures such as k-dimensional trees and particle filtering. Results of several validation experiments are presented.

1 INTRODUCTION

Nowadays a structured and fruitful Human-Robot Interaction (HRI) represents the key factor that will facilitate industrial robots to be massively used in SMEs. Obviously, in order to allow an efficient HRI, physical separation of robot and human workspaces must be overcome and safety fences must be removed. This lack of artificially imposed safety must be compensated for by endowing robot control systems with more advanced safety functionalities, like for instance Human Detection and Tracking (HDT).

The problem of HDT consists in detecting the presence of one or more human beings inside a specific environment and track their motion (in terms of position and, if possible, velocity) on the basis of a series of consecutive "descriptions" of the supervised scene provided by one or more sensors. As a matter of fact, knowing if a human worker has entered a robotic cell and being able to follow his/her motion would allow the control system to choose the most suitable control strategy in order to avoid collisions (by keeping the robot as distant as possible from the human) or to allow safe HRI (by enforcing a compliant behaviour of the manipulator).

In this context the most typical choice is to use surveillance RGB cameras (especially fish-eye cameras), since they are both convenient and easily deployable, but depth sensors or mixed RGB-D sensors (like for instance Microsoft Kinect ®) can be used as well.

1.1 State of the Art

Although HDT can be used in several contexts, we will address only its use in industrial robotics. Techniques to perform HDT in an industrial environment using respectively a single camera or multiple cameras are described in (Rogez et al., 2014) and (Elshafie and Bone, 2008), while high-visibility industrial clothing detection strategies based on RGB and IR cameras have been proposed in (Mosberger and Andreasson, 2013) and (Mosberger et al., 2013). Approaches based on pressure-sensitive sensors mounted on the floor have been proposed as well, like for instance (Najmaei et al., 2011). Finally examples of HDT relying on RGB-D sensor can be found in (Munaro et al., 2012) and (Munaro et al., 2013).

Sometimes the problem of HDT has been tackled simultaneously with the problem of predicting online the motion and/or the trajectory followed by a human (also known as Human Intention Estimation). In (Kulić and Croft, 2007) techniques combining vision and psychological signal measurement for human motion estimation during HRI are presented, while (Asaula et al., 2010) describe a system for pre-

Ragaglia M., Bascetta L. and Rocco P..
Multiple Camera Human Detection and Tracking Inside a Robotic Cell - An Approach based on Image Warping, Computer Vision, K-d Trees and Particle Filtering.
DOI: 10.5220/0005045703740381
In *Proceedings of the 11th International Conference on Informatics in Control, Automation and Robotics* (ICINCO-2014), pages 374-381
ISBN: 978-989-758-040-6
Copyright © 2014 SCITEPRESS (Science and Technology Publications, Lda.)

dicting the probability of an accident in a HRI industrial scenario based on a dynamic stochastic model of the human motion. Finally, (Bascetta et al., 2011) present a strategy, based on HDT, to estimate the destination of a human walking inside a robotic cell.

1.2 Main Contributions and Outline

In this paper we propose a solution to HDT organised in a pipeline of different steps. Starting from a scene monitored by multiple RGB surveillance cameras, the different RGB images are acquired and warped together to create a unique combined image. Background/Foreground Segmentation (BG/FG Segmentation) is applied to the combined image to detect human workers. K-dimensional trees data structures (k-d trees) are then used to efficiently update in time the information regarding humans' silhouettes detected via BG/FG Segmentation. Finally multiple Particle Filters perform the tracking functionality.

With respect to the previously mentioned state of the art, the main contributions of this work can be summarized as follows:

- **Image Fusion**: multiple images simultaneously acquired from different surveillance cameras are warped together to obtain a unique combined image describing the whole supervised environment;
- **Abstraction from Physical Sensors**: Image Fusion completely decouples the HDT processing pipeline from physical sensors. Though multiple physical cameras are used, the HDT pipeline "sees" only one logical sensor from which the combined image is acquired;
- **K-d Trees**: the use of k-d trees provides an efficient and elegant solution to the problem of updating in time the information regarding detected human workers;

The remainder of this work is organized as follows. Section 2 describes the image warping techniques used for image fusion, while the BG/FG Segmentation algorithm is presented in Section 3. The usage of k-dimensional tree data structure is covered in Section 4 and the adopted particle filtering strategy is described in Section 5. Finally Section 6 shows the results obtained from several validation experiments.

2 MULTIPLE CAMERAS IMAGE FUSION

The fusion of images acquired from R different cameras relies on calibration of every vision sensor. For every available surveillance camera both the intrinsic and the extrinsic calibration matrices, respectively I_r and E_r, are identified. While I_r maps the r-th camera Cartesian frame to the r-th camera pixel coordinate frame, E_r maps 3D points expressed in the world-base Cartesian frame to the r-th camera Cartesian frame, as sketched in Figure 1. Moreover, also the radial and tangential distortion coefficients d_r are identified:

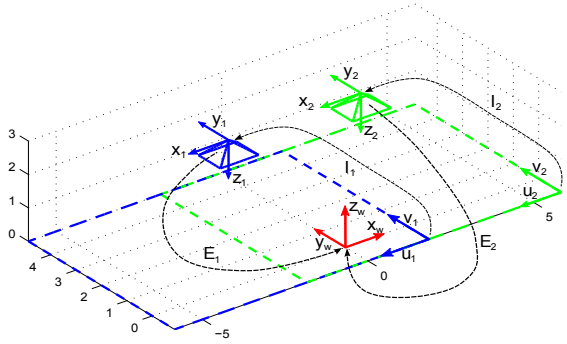

Figure 1: Example of a setup including two calibrated cameras and corresponding image planes.

$$d_r = \{k_{1r},\ k_{2r},\ p_{1r},\ p_{2r},\ k_{3r}\} \quad (1)$$

In order to obtain a unique image describing the whole supervised environment, images acquired from several surveillance cameras must be compensated for distortion effects (using d_r) and then they must be warped together. Image warping consist in mapping every pixel P_o in the original image to a different pixel P_w through a warping matrix W:

$$P_w = [u_w, v_w]^T = W\ P_o = W\ [u_o, v_o]^T \quad (2)$$

A reference camera is selected so that the coordinate transform between the world frame and the combined image pixel coordinate frame (and viceversa) can be described by the extrinsic and intrinsic calibration matrices of the reference camera. At this point images must be warped together in such a way that pixels describing corresponding points on the floor plane can be exactly overlapped. To obtain this result the homography matrix H_r of the r-th (non-reference) camera image plane with respect to the reference camera image plane must be identified, with both image planes corresponding to the scene floor.

Since H_r is a 3x3 matrix defined up to a scale factor, the problem of identifying its elements can be solved by considering four corresponding points between the reference camera image and the r-th camera image. In order to find the homography matrices that map the r-th camera image plane to the reference camera image plane while preserving the scene floor, four different points P_i^W belonging to the scene floor ($z_i^W = 0$) are chosen and mapped to both the reference camera and the r-th camera pixel coordinate

frame (p_i^{ref} and p_i^r respectively):

$$\forall i \in [1,4]\ P_i^W = \left[x_i^W, y_i^W, 0, 1\right]^T \quad (3)$$

$$P_i^{ref} = E_{ref} P_i^W = \left[x_i^{ref}, y_i^{ref}, z_i^{ref}, 1\right]^T \quad (4)$$

$$P_i^r = E_r P_i^W = [x_i^r, y_i^r, z_i^r, 1]^T \quad (5)$$

$$p_i^{ref} = I_{ref} \left[x_i^{ref}/z_i^{ref}, y_i^{ref}/z_i^{ref}, 1\right]^T \quad (6)$$

$$p_i^r = I_r \left[x_i^r/z_i^r, y_i^r/z_i^r, 1\right]^T \quad (7)$$

Finally, to determine the r-th homography matrix H_r so that:

$$p_i^{ref} = H_r\ p_i^r \quad i \in [1,4] \quad (8)$$

the procedure described in (Hartley and Zisserman, 2004) is followed. Since surveillance cameras are fixed, the identification of homograpy matrices H_r can be performed entirely offline so that the warping stage of the HDT pipeline simply warps every acquired image using the corresponding homography and overlaps the warped images to obtain the combined image, as shown in Figure 2.

3 HUMAN DETECTION VIA BG/FG SEGMENTATION

Having warped together all the images acquired by the different RGB surveillance cameras, it is possible to perform BG/FG Segmentation on the combined image in order to detect human beings entering the robotic cell or walking inside it.

3.1 BG/FG Segmentation Algorithm

The BG/FG Segmentation algorithm adopted in this work is part of the OpenCV library (Bradski, 2000) and it is described in (Zivkovic, 2004) and (Zivkovic and Van Der Heijden, 2006). It consists in an efficient adaptive algorithm that performs background subtraction at pixel level and that relies on Gaussian mixture probability density. It also offers the possibility to trigger online background update. As shown in Figure 3, the algorithm's output consists in two different images:

- **Foreground Mask**: binary image whose pixels are white (black) if the corresponding pixel of the input image belongs to the foreground (background);
- **Foreground Image**: RGB colour image containing only the foreground pixels. It is obtained by simply applying the binary mask to the input image.

Moreover the algorithm provides a shadow detection functionality (KaewTraKulPong and Bowden, 2002) that allows to perform object detection while discarding shadows of segmented objects.

3.2 BG/FG Segmentation Post-processing

After BG/FG Segmentation, the Foreground Mask is further processed performing "image opening", i.e. applying in sequence an erosion and a dilation kernel (Bradski and Kaehler, 2008). The main advantage brought by applying image opening to the Foreground Mask consists in removing image noise (especially isolated pixels erroneously classified as foreground) while preserving large foreground areas.

At this point the contours of the connected components in the Foreground Mask image are extracted and a last "plausibility check" is introduced. As a matter of fact it is reasonable to assume that foreground areas must be large enough to represent a human being walking inside the scene. Consequently if a foreground area's surface (measured in square pixels) is smaller than an experimentally determined threshold value, the object is considered a false positive and it is discarded. Otherwise it is actually classified as a detected human worker.

4 USING K-d Trees TO UPDATE DETECTED HUMANS

The main problem related to the output of BG/FG Segmentation stage is to determine for every foreground area detected at time step i, the corresponding area inside the foreground image computed at time step $i-1$. As a matter of fact a continuous update of the contours of the silhouette describing the same human being across a series of consecutive time instants is fundamental to feed the different particle filters with coherent information (see Section 5). To solve this issue the information regarding detected humans is structured in k-d trees, but first the following "plausibility hypotheses" are considered:

- humans cannot suddenly appear inside the robotic cell or either disappear from it;
- humans can enter/exit the cell only through one or more access areas (i.e. gates, doors, ecc.);
- it is likely that the position of the same human being will undergo limited variations from one time step to the following one.

SCITEPRESS SCIENCE AND TECHNOLOGY PUBLICATIONS

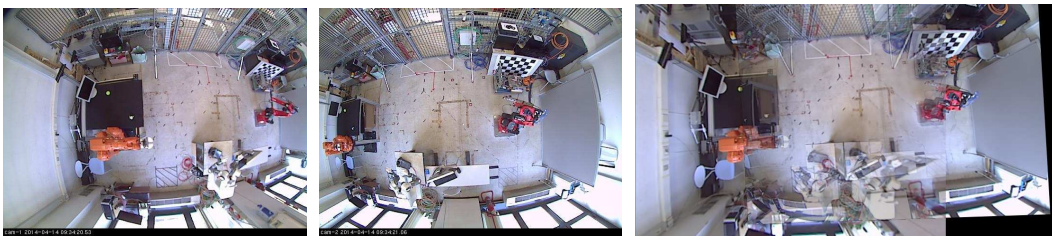

(a) (b) (c)

Figure 2: Example of multiple camera image fusion. Left: image acquired from camera #01. Middle: image acquired from camera #02. Right: combined image resulting from image fusion.

(a) (b) (c)

Figure 3: Example of Single Camera BG/FG Segmentation. Left: input image. Middle: foreground mask. Right: foreground image.

SCIENCE AND TECHNOLOGY PUBLICATIONS

Thanks to these hypotheses the problem of erroneous robot detection can be easily overcome: even if a moving industrial robot is detected by BG/FG Segmentation, it won't be considered as a human being. While (Bascetta et al., 2011) tackled this problem by masking out the entire robot's workspace inside the Foreground Image, the approach here presented does not require this further image-processing step and avoids large parts of the acquired image to be ignored, thus resulting simpler, more efficient and more effective.

4.1 K-d Trees

A k-d tree (or k-dimensional tree) is a space-partitioning data structure that allows to organize points belonging to a k-dimensional space (Moore, 1991) in a binary tree. Considering a variant of k-d trees, where actual points can be stored only in the leaf nodes, every non-leaf node represents a splitting hyperplane that divides the k-d space into two half-spaces. Points to the left of this hyperplane are represented by the left subtree of that node and points right of the hyperplane are represented by the right subtree. An example of a 2-dimensional tree is shown in Figure 4.

4.2 Detected Humans' Update via Nearest Neighbour Search

Using k-d trees the problem of updating online the

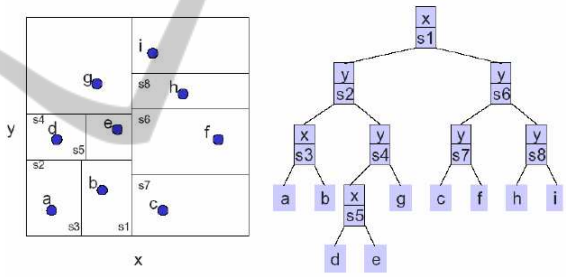

Figure 4: Example of k-d tree where non-leaf nodes represent splitting hyperplanes and leaf nodes consist in actual 2-dimensional points.

information regarding detected humans can be elegantly formalized as the identification of couples of nearest neighbours between two different 2-d trees: one (named `FG_previous`) containing the Center-of-Gravity (CoG) of the human silhouettes detected on the combined image at the previous time step and another one (named `FG_now`) containing the CoG of the foreground areas segmented at the current time step. The following pseudo-code explains how this nearest neighbour search can be performed:

```
for(f_now in FG_Now)
   f_prev := nearest(FG_Previous, f_now)
   if f_now == nearest(FG_Now, f_prev)
      add (f_prev, f_now) to results
   end if
end for
```

Not only this solution is very elegant, but it is also

very efficient. If we suppose that both sets contain n elements, the time complexity of building the corresponding 2-d trees and searching for couples of nearest neighbours is $O(n\,logn)$, while the time complexity of performing distance checks between every possible pair of elements would be $O(n^2)$.

After identifying the couples of nearest neighbours between the two 2-d trees, two last checks are performed: every foreground area detected near an entrance zone, but not associated to a previously detected human, is considered as a new human entering the cell, and every detected human no longer associated to a foreground area is considered as a person that left the cell.

5 HUMAN TRACKING VIA PARTICLE FILTERING

The tracking strategy here adopted is inspired by the one proposed in (Bascetta et al., 2011). After BG/FG Segmentation and foreground areas update, human workers are tracked by a series of particle filters that rely on a simplified human walking motion model. The choice of both the motion model and the particle filtering strategy results from the following assumptions:

- the scene consists of a flat ground plane on which humans walk around;
- a human worker does not walk sideways;
- human workers and industrial robots are the unique moving objects in the camera field of view, but, since robots do not enter the scene from the entrance zones, their detection is automatically avoided.

5.1 Human Motion Model

A simple and effective way of tracking a human being motion consists in considering his/her volumetric occupancy. By circumscribing a rectangular box around a walking person, we are able to describe his/her motion in terms of translation on the floor and rotation around the vertical axis crossing the base in its centre (see Figure 5(a)).

Having fixed on the ground plane a world-base Cartesian frame, the pose of a human can be completely described as $p = (x, y, \theta)$, where x and y are the box base coordinate with respect to the world base frame X-axis and Y-axis respectively and θ is the angle formed between the tangent to the walking path and the world base frame X-axis.

Finally, according to the assumption that both the linear velocity v (i.e. the nonholonomic velocity along the direction of motion) and the angular velocity ω are piece-wise constant, the adopted human walking dynamic model can be rendered as a slightly modified version of the unicycle model presented in (Arechavaleta et al., 2008):

$$\begin{cases} \dot{x} &= v\cos(\theta) \\ \dot{y} &= v\sin(\theta) \\ \dot{\theta} &= \omega \\ \dot{v} &= \sigma \\ \dot{\omega} &= \eta \end{cases} \tag{9}$$

where σ and η are two independent and uncorrelated Gaussian white noises acting respectively on the linear velocity v and on the angular velocity ω.

5.2 Particle Filtering Strategy

In our scenario deterministic evaluation of the human motion state is not possible mainly because of significant measurement noise. Moreover, analytical calculation of the motion model output in terms of multiple rectangular boxes (each one projected according to a single camera point of view) is not feasible.

Consequently, our tracking strategy consists in assigning to every detected human a probability distribution over the possible states in the form of a set weighted particles, propagated in time according to the motion model presented in Section 5.1. In this way, for every moving worker, multiple virtual representations are generated and his/her motion state is estimated by selecting the particle whose representation best matches the measured foreground. At any time instant i the motion state of a single walking human being is composed by a set of N particles:

$$Q_i = \left\{ q_i^{(j)} \mid j = 1,\ldots,N \right\} \tag{10}$$

where every particle represents a possible motion state configuration:

$$q_i^{(j)} = \left(x_i^{(j)}, y_i^{(j)}, \theta_i^{(j)}, v_i^{(j)}, \omega_i^{(j)} \right) \tag{11}$$

The initial distribution can be considered known a priori and it corresponds to a scene without moving workers. Right after instantiation, every filter is considered "inactive" and its particle set is initialised via uniform random sampling inside a subspace of the model state space defined around the entrance areas. As soon as a new human is detected (see Section 3), an "inactive" filter is assigned the corresponding foreground area and thus, it becomes "active".

While receiving continuously updated information regarding the foreground area it is tracking (see

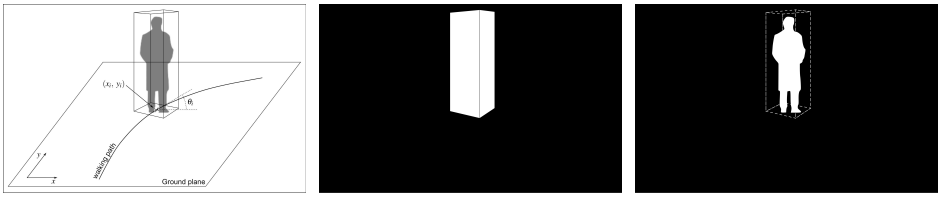

(a) (b) (c)

Figure 5: Left: human worker detected silhouette (grey), pose and circumscribed box according to the explained motion model. Middle: graphic output of a particle motion model state considering a single camera. Right: pixel determining the particle's value considering a single camera.

Section 4), the particle filter keeps propagating particles. Naming f the transfer function corresponding to the discrete motion model, the particle set propagation from time step i to time step $i+1$ can be simply defined as:

$$Q_{i+1} = \left\{ q_{i+1}^{(j)} = f\left(q_i^{(j)}\right) \mid j = 1,\ldots,N \right\} \quad (12)$$

The probability that each particle corresponds to the actual state of the walking human is computed on the basis of two binary images: the first contains the foreground area describing the human appearance (see Figure 5(c)), the latter represents the appearance of the particle itself. The box vertices are computed on the basis of the particle and projected in every camera perspective. A binary image is created where non-zero pixels belong to the superposition of the box projections (see Figure 5(b)). The probability measure is finally obtained by counting the number of non-zero pixels contained in the logic AND of the two binary images, as depicted in Figure 5(c). After evaluation, particles probabilities are normalised using their sum $\bar{\alpha}_i = \sum_{j=1}^{N} \alpha_i^{(j)}$ as a normalizing factor:

$$\alpha_i^{(j)} := \alpha_i^{(j)} / \bar{\alpha}_i, \ \forall j \in [1,\ldots,N] \quad (13)$$

To update the estimate of the human state, a best particle is extracted from the filter's particle set. Particles are sorted in descending order with respect to probability values and the best particle is computed as the weighted average of the best n particles (i.e. the first n particles within the sorted set).

The re-sampling stage realizes a balance between exploitation and exploration. Particles being the nearest with respect to the actual state of the walking human are mixed to new particles obtained via uniform random sampling inside a subspace of the model state space defined around the best particle previously extracted.

Finally, when the tracked human being exits the supervised environment, the filter goes back to the "inactive" state and waits until it is assigned another human to track. The design and implementation of the filtering stage has been realized so that the number M of particle filters running in parallel, the dimension N of each filter particle set, the number n of particles to average during best particle extraction and the percentage of maintained particles can be configured by the user prior to the actual execution.

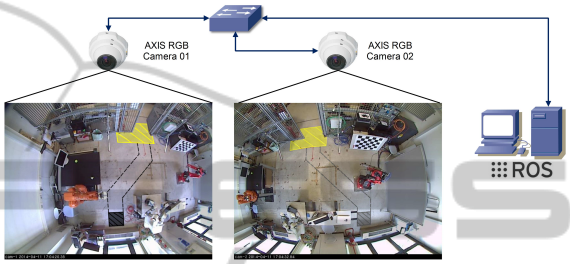

Figure 6: The experimental setup comprising the two AXIS fish-eye surveillance cameras, the PC running the HDT application and the Ethernet connection between the different components. The entrance area is highlighted in yellow and the two walking paths and the corresponding destination areas are highlighted respectively in black and grey.

6 EXPERIMENTAL RESULTS

Experimental validation of the proposed HDT approach has been performed in our laboratory. The experimental setup depicted in Figure 6 includes three industrial robots (an ABB IRB140, an ABB FRIDA prototype robot and a COMAU Smart-Six) and two AXIS 212 PTZ RGB Network cameras connected via Ethernet to the PC hosting both the ROS network and the HDT application. Walking paths and destination areas have been drawn on the floor in order to provide ground-truth for the experiments described in the following.

The particle filters' parametrization adopted during the experiments was the following:

- 3 particle filters running in parallel;
- 250 particles composing each particle set;
- best particle extraction via weighted average of the 1% best particles;

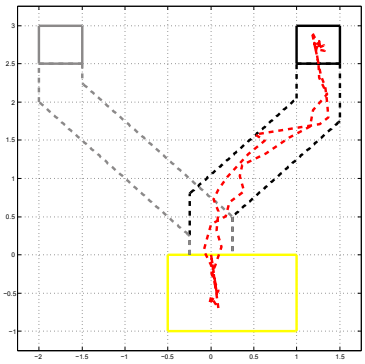

Figure 7: Graph showing that the human position estimate computed by the HDT System (dashed red) is always included inside the path drawn on the ground (dashed black).

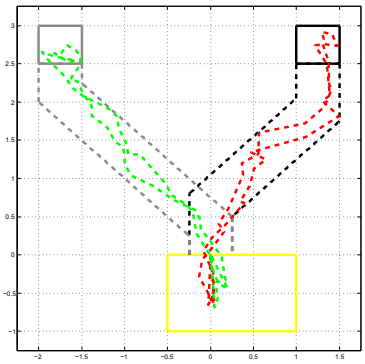

Figure 8: Graph showing that the human worker position estimates computed by the HDT System (dashed red and dashed green) are always included inside the corresponding paths drawn on the ground (respectively dashed black and dashed grey).

- 20% best particles maintained during resampling.

6.1 Experiment #1: Single Person Detection and Tracking

In the first experiment a human worker enters the robotic cell and reaches the destination area #1 (the one coloured in black in Figure 6) following the path defined by the black dotted lines drawn on the floor. Considering the drawn black path as ground-truth, Figure 7 demonstrates the effectiveness of our approach to HDT by showing that the best particle two-dimensional position (i.e the human worker trajectory estimated by the particle filter) is always included in the area delimited by the black dotted lines.

6.2 Experiment #2: Multiple Person Detection and Tracking

During the second experiment two human workers enter the robotic cell. The first directs himself towards destination area #1, following the path drawn in black, while the latter reaches destination area #2, following the path defined by grey dotted lines. Figure 8 shows once again that the trajectories followed by the two human workers estimated by the particle filters are always included in the area delimited by the drawn dotted lines.

7 CONCLUSIONS

The paper discusses an approach to Human Detection and Tracking in a robotic cell. The proposed solution is characterized by fusion of images coming from multiple fish-eye RGB surveillance cameras into a unique image that is fed to a BG/FG Segmentation algorithm. K-d trees are used to store and update information regarding detected humans in time. Finally a series of particle filters, based on a human motion model, are used to track detected humans. Software engineering aspects are discussed and experimental results are presented.

The HDT approach presented in this paper lends itself to several future developments:

- integration of different kind of sensors (like for instance range finders or RGB-D sensors) that will possibly allow to exploit more sophisticated kinematic models of the human motion;
- integration of fine-grained geometric models of the manipulators installed inside the cell to completely mask their motion and definitively avoid their detection via BG/FG Segmentation;
- development of a suitable interface to directly send the information computed by HDT to a standard robot controller.

REFERENCES

Arechavaleta, G., Laumond, J.-P., Hicheur, H., and Berthoz, A. (2008). An optimality principle governing human walking. *Robotics, IEEE Transactions on*, 24(1):5–14.

Asaula, R., Fontanelli, D., and Palopoli, L. (2010). Safety provisions for human/robot interactions using stochastic discrete abstractions. In *Intelligent Robots and Systems (IROS), 2010 IEEE/RSJ International Conference on*, pages 2175–2180.

Bascetta, L., Ferretti, G., Rocco, P., Ardo, H., Bruyninckx, H., Demeester, E., and Di Lello, E. (2011). Towards safe human-robot interaction in robotic cells: An approach based on visual tracking and intention estimation. In *Intelligent Robots and Systems (IROS), 2011*

IEEE/RSJ International Conference on, pages 2971–2978.

Bradski, G. (2000). The OpenCV Library. *Dr. Dobb's Journal of Software Tools*.

Bradski, G. and Kaehler, A. (2008). *Learning OpenCV: Computer Vision with the OpenCV Library*. O'Reilly Media.

Elshafie, M. and Bone, G. (2008). Markerless human tracking for industrial environments. In *Electrical and Computer Engineering, 2008. CCECE 2008. Canadian Conference on*, pages 001139–001144.

Hartley, R. I. and Zisserman, A. (2004). *Multiple View Geometry in Computer Vision*. Cambridge University Press, ISBN: 0521540518, second edition.

KaewTraKulPong, P. and Bowden, R. (2002). An improved adaptive background mixture model for real-time tracking with shadow detection. In Remagnino, P., Jones, G., Paragios, N., and Regazzoni, C., editors, *Video-Based Surveillance Systems*, pages 135–144. Springer US.

Kulić, D. and Croft, E. (2007). Pre-collision safety strategies for human-robot interaction. *Auton. Robots*, 22(2):149–164.

Moore, A. (1991). A tutorial on kd-trees. Extract from PhD Thesis. Available from `http://www.ri.cmu.edu/pub_files/pub1/moore_andrew_1991_1/moore_andrew_1991_1.pdf`.

Mosberger, R. and Andreasson, H. (2013). An inexpensive monocular vision system for tracking humans in industrial environments. In *Robotics and Automation (ICRA), 2013 IEEE International Conference on*, pages 5850–5857.

Mosberger, R., Andreasson, H., and Lilienthal, A. (2013). Multi-human tracking using high-visibility clothing for industrial safety. In *Intelligent Robots and Systems (IROS), 2013 IEEE/RSJ International Conference on*, pages 638–644.

Munaro, M., Basso, F., and Menegatti, E. (2012). Tracking people within groups with rgb-d data. In *Intelligent Robots and Systems (IROS), 2012 IEEE/RSJ International Conference on*, pages 2101–2107.

Munaro, M., Lewis, C., Chambers, D., Hvass, P., and Menegatti, E. (2013). Rgb-d human detection and tracking for industrial environments. In *13th International Conference on Intelligent Autonomous Systems (IAS-13)*. accepted.

Najmaei, N., Kermani, M., and Al-Lawati, M. (2011). A new sensory system for modeling and tracking humans within industrial work cells. *Instrumentation and Measurement, IEEE Transactions on*, 60(4):1227–1236.

Rogez, G., Orrite, C., Guerrero, J., and Torr, P. H. (2014). Exploiting projective geometry for view-invariant monocular human motion analysis in man-made environments. *Computer Vision and Image Understanding*, 120(0):126 – 140.

Zivkovic, Z. (2004). Improved adaptive gaussian mixture model for background subtraction. In *Pattern Recognition, 2004. ICPR 2004. Proceedings of the 17th International Conference on*, volume 2, pages 28–31 Vol.2.

Zivkovic, Z. and Van Der Heijden, F. (2006). Efficient adaptive density estimation per image pixel for the task of background subtraction. *Pattern Recogn. Lett.*, 27(7):773–780.

SCITEPRESS SCIENCE AND TECHNOLOGY PUBLICATIONS